

## Intense Geodesic Acousticlike Modes Driven by Suprathermal Ions in a Tokamak Plasma

R. Nazikian,<sup>1</sup> G. Y. Fu,<sup>1</sup> M. E. Austin,<sup>2</sup> H. L. Berk,<sup>2</sup> R. V. Budny,<sup>1</sup> N. N. Gorelenkov,<sup>1</sup> W. W. Heidbrink,<sup>3</sup> C. T. Holcomb,<sup>4</sup> G. J. Kramer,<sup>1</sup> G. R. McKee,<sup>5</sup> M. A. Makowski,<sup>4</sup> W. M. Solomon,<sup>1</sup> M. Shafer,<sup>5</sup> E. J. Strait,<sup>6</sup> and M. A. Van Zeeland<sup>6</sup>

<sup>1</sup>Princeton Plasma Physics Laboratory, Princeton, New Jersey 08543, USA

<sup>2</sup>University of Texas at Austin, Austin, Texas 78712, USA

<sup>3</sup>University of California Irvine, Irvine, California 92697, USA

<sup>4</sup>Lawrence Livermore National Laboratory, Livermore, California 94550, USA

<sup>5</sup>University of Wisconsin-Madison, Madison, Wisconsin 53706, USA

<sup>6</sup>General Atomics, San Diego, California 92186-5608, USA

(Received 24 June 2008; published 30 October 2008)

Intense axisymmetric oscillations driven by suprathermal ions injected in the direction counter to the toroidal plasma current are observed in the DIII-D tokamak. The modes appear at nearly half the ideal geodesic acoustic mode frequency, in plasmas with comparable electron and ion temperatures and elevated magnetic safety factor ( $q_{\min} \geq 2$ ). Strong bursting and frequency chirping are observed, concomitant with large (10%–15%) drops in the neutron emission. Large electron density fluctuations ( $\tilde{n}_e/n_e \approx 1.5\%$ ) are observed with no detectable electron temperature fluctuations, confirming a dominant compressional contribution to the pressure perturbation as predicted by kinetic theory. The observed mode frequency is consistent with a recent theoretical prediction for the energetic-particle-driven geodesic acoustic mode.

DOI: 10.1103/PhysRevLett.101.185001

PACS numbers: 52.35.Bj, 52.50.Gj, 52.55.Fa, 52.65.Ww

A key goal of a future deuterium-tritium burning plasma experiment such as ITER [1] is to explore the accessibility of steady state reactor regimes in plasmas that are predominantly self-heated by 3.5 MeV alpha particles [2]. A significant issue for such regimes is whether alpha particles (together with suprathermal  $\sim 1$  MeV beam ions injected into the plasma) will undergo collective oscillations with detrimental effects on fast ion confinement. The role of present fusion experiments is, in part, to develop predictive tools for assessing collective fast ion phenomena in steady state reactor regimes [3]. High energy hydrogenic beams are a widely used source of plasma heating in present fusion experiments. These beams are typically injected in the direction of the plasma current (cobeam injection) in order to capture the beam ions on well confined orbits for efficient central plasma heating [4]. As a consequence, extensive studies have been performed on Alfvén wave excitation using coinjected beam ions [5–11]. However, comparatively little effort has been invested in exploring instabilities driven by suprathermal ions injected counter to the direction of the plasma current.

In this Letter we show the surprising result that counterbeam injection excites intense axisymmetric oscillations that are not readily observed in comparable cobeam injection plasmas on DIII-D [10,12] or JET [9,13]. The mode activity exhibits bursting and frequency chirping concomitant with sharp drops in the neutron emission, indicative of strong beam ion redistribution and/or loss. The mode frequency is  $\sim 50\%$  below the ideal geodesic acoustic mode (GAM) frequency [14,15]. The modes occur in plasmas with elevated central magnetic safety factor ( $q_{\min} \geq 2$ ) and with comparable ion and electron temperatures, relevant to

steady state plasma regimes. A theoretical analysis [16] identifies a new nonperturbative beam driven instability, the energetic particle GAM (E-GAM), that arises at a frequency well below the standard GAM frequency [17]. A new fluid-kinetic hybrid model using the measured DIII-D equilibrium profiles, including beam ions on counterpassing orbits, qualitatively replicates the mode characteristics in the experiment [16].

Figure 1 shows a typical example of an axisymmetric ( $n = 0$ ) mode excited in DIII-D during counterbeam injection. 75 keV deuterium beams are injected into the plasma during the ramp-up phase of the toroidal plasma current [Fig. 1(a)], resulting in mode bursting [Fig. 1(b)] and frequency chirping [Fig. 1(c)] on magnetic pickup probes located external to the plasma. Each burst is only of a few milliseconds in duration and is accompanied by 10%–15% drops in the 2.5 MeV neutron emission [Fig. 1(b)]. The neutron emission is predominantly due to beam ion collisions with the background plasma [ $D + D \rightarrow n(2.5 \text{ MeV}) + {}^3\text{He}$ ], and is thus proportional to the fast ion population. The neutron drops commence at the start of the frequency chirps and no other mode activity occurs in conjunction with the  $n = 0$  mode. The rapid bursting and frequency chirping is characteristic of hole-clump generation in the beam ion velocity distribution [18,19]. The magnetic field fluctuations measured at the wall are particularly weak ( $\tilde{B}_\theta/B \approx 10^{-5}$ ) and have a clear  $n = 0$  mode pattern.

Beam emission spectroscopy (BES) [20] and electron cyclotron emission (ECE) were used to map the internal density and temperature mode structure. The equilibrium safety factor ( $q$  profile) was mapped using the motional

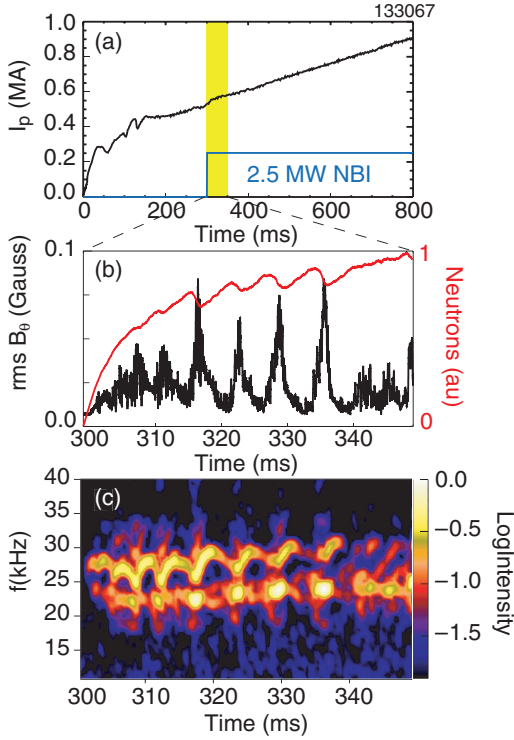


FIG. 1 (color). Evolution of (a) plasma current  $I_p$  and 75 keV deuterium neutral beam power  $P_{\text{NBI}}$ , (b) edge poloidal magnetic field fluctuations  $\tilde{B}_\theta$  and neutron emission  $n_s$ , (c) time resolved power spectrum of  $\tilde{B}_\theta$ . Bursting and frequency chirping coincide with 10%–15% drops in the neutron emission. Plasma toroidal magnetic field  $B_T = 2$  T, major radius  $R_0 = 1.7$  m, minor radius  $a = 0.6$  m.

stark effect (MSE) diagnostic [21]. Figure 2(a) shows the radial profile of the rms electron density fluctuation obtained by integrating over the frequency bandwidth of the mode. The density fluctuation level is measured along a 16 channel BES radial array 12 cm in extent and located 6 cm above the plasma midplane. The profile is obtained from a composite of three reproducible discharges where the array was scanned radially between discharges. The data show a broad density mode structure with rapid fall off at large radius. This is inconsistent with the highly localized structure expected near the magnetic axis for the ideal GAM [14]. No detectable electron temperature fluctuations were observed down to the ECE noise floor of 0.2% corresponding to the yellow band in Fig. 2(a). Phase measurements between successive BES channels indicate very long wavelengths in the poloidal and radial direction, well within the spatial resolution of the ECE diagnostic. The large discrepancy between electron density and temperature fluctuations is inconsistent with shear Alfvén wave observations in DIII-D [10]. From kinetic theory, the electrons should remain isothermal along the magnetic field lines for low frequency modes due to the large electron poloidal transit frequency (400 kHz for  $q_{\text{min}} = 3$  and  $T_e = 1$  keV in Fig. 2). Hence, for low frequency shear Alfvén waves it

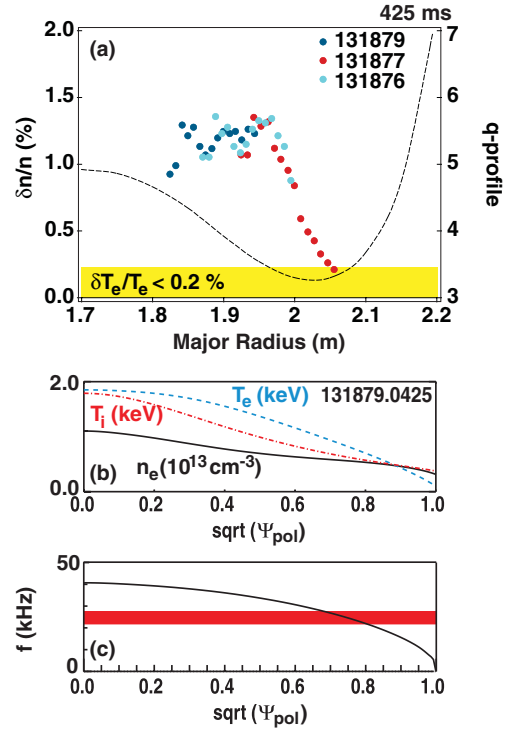


FIG. 2 (color). Radial profiles of (a) the density fluctuation level  $\tilde{n}_e/n_e$  and  $q$  profile vs major radius  $R$  measured using beam emission spectroscopy (BES), taken 6 cm above the plasma midplane; (b) ion temperature  $T_i$ , electron temperature  $T_e$ , electron density  $n_e$  vs  $\sqrt{\Psi_{\text{pol}}}$  where  $\Psi_{\text{pol}}$  is the poloidal flux; (c)  $n = 0$  GAM continuum evaluated using the NOVA code and the observed range of frequency (red band).  $B_T = 2$  T,  $R_0 = 1.7$  m.

is the dominant radial component of the  $E \times B$  motion that gives rise to comparable electron density and electron temperature perturbation. In contrast, the data in Fig. 2(a) are consistent with a dominant  $E \times B$  motion tangential to the flux surfaces (induced by radial electric fields) with negligible radial displacement. A consequence is a dominant compressional contribution to the electron density fluctuations with relatively weak electron temperature and poloidal magnetic field fluctuations.

The NOVA code [22], which includes geodesic acoustic mode (electrostatic) coupling to shear Alfvén waves [23,24], was used to calculate the  $n = 0$  GAM continuum, shown in Fig. 2(c). The GAM continuum is calculated using the effective adiabatic index  $\gamma = (P_e + 7/4P_i)/(P_e + P_i + P_f) \approx 0.81$  where  $P/\rho^\gamma = c$ ,  $P$  is the total plasma pressure,  $P_i$ ,  $P_e$ ,  $P_f$  are the ion, electron, and fast ion pressure,  $\rho$  in the mass density, and  $c$  is a constant. Off-axis peaking of the GAM continuum is a requirement for the existence of the ideal GAM and such conditions may be achieved in JET with strong magnetic shear reversal [14,25]. In contrast, the GAM continuum rarely peaks off-axis in DIII-D due to weak magnetic shear reversal and monotonic temperature profiles. Extensive NOVA

analysis confirms that no ideal GAM solution exists for these DIII-D discharges.

However, a newly developed nonperturbative electrostatic theory for the energetic-particle-driven GAM, the E-GAM, captures many of the features observed in experiment [16]. The analysis shows that a robust  $n = 0$  mode with dominant radial electric field and a GAM-like  $m = 1$  density perturbation [14], can be driven well below the ideal GAM frequency when the energetic particle pressure is a significant fraction of the thermal plasma pressure. The mode frequency occurs below the poloidal transit frequency of the injected beam ions and is driven unstable by beam ion anisotropy. The mode radial width is determined by the drift orbit width of the passing ions, which increases with increasing magnetic safety factor. For 75 keV counterinjected beam ions with  $q_{\min} \approx 3.5$  [Fig. 2(a)], the poloidal transit frequency of the beam ions is close to 45 kHz, or about  $2\times$  the observed mode frequency. Both the velocity anisotropy and drift orbit width are largest for counterpassing particles at high  $q_{\min}$  in DIII-D [4], consistent with the conditions for the observation of mode activity.

The E-GAM is simulated using a hybrid model with a fluid description for the thermal plasma and a drift kinetic description for the fast ions [16]. Linear simulations have been carried out using a slowing down distribution for the injected beam ions for the profiles corresponding to the DIII-D discharge in Fig. 2. Figure 3(a) shows the electron density perturbation  $\tilde{n}_e/n_e$  calculated using the hybrid code with a beam ion beta on axis,  $\beta_h(0) = 0.17\%$ , and fast ion profile corresponding to classical orbit analysis using the TRANSP code [26]. The fast ion beta is comparable to the thermal plasma beta [ $\beta_{th}(0) = 0.13\%$ ] within 100 ms of the start of beam injection, corresponding to the plasma profiles shown in Fig. 2. The calculated electron density perturbation is global, consistent with observations on DIII-D [Fig. 2(a)], and unlike the core localized structure expected for the ideal GAM [14]. Figure 3(b) shows the simulation results for the mode frequency and growth rate vs  $\beta_h(0)$ . The simulation result in Fig. 3(b) indicates that the mode frequency is largely independent of  $\beta_h(0)$  near

( $\approx 20$  kHz). This is close to the observed mode frequency (22–28 kHz) and well below the poloidal transit frequency of the 75 keV counterpassing beam ions ( $\approx 45$  kHz). From theory the E-GAM frequency scales with the poloidal transit frequency of the beam ions which scales inversely with  $q_{\min}$ , consistent with observations. The simulations also indicate a very large linear growth rate [Fig. 3(b)] up to  $\gamma/\omega \approx 30\%$ . The fast ion beta for mode onset extrapolates to  $\beta_h(0) \approx 0.05\%$ , consistent with the early onset of the instability in experiment [Fig. 1(c)]. The elevated  $q_{\min}$  allows GAM-like modes to arise without substantial thermal ion Landau damping, leading to a low  $\beta_h(0)$  threshold for the mode onset. The large linear growth rates calculated

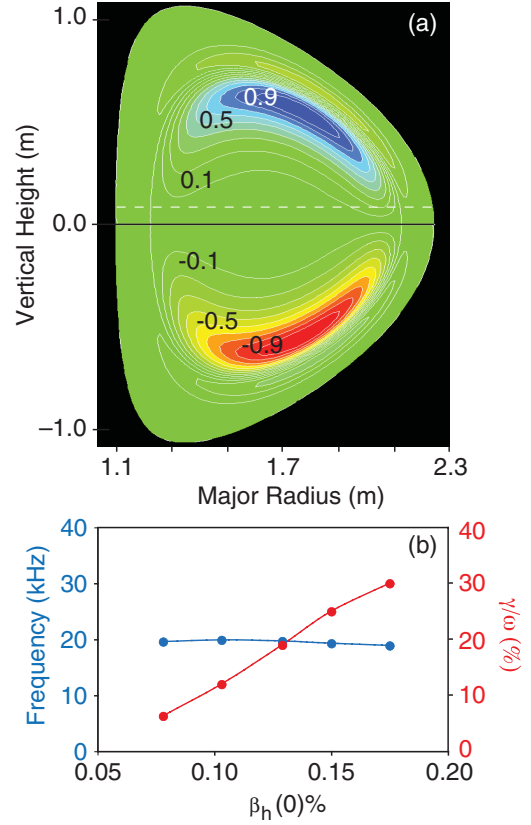


FIG. 3 (color). (a) 2D density perturbation ( $\tilde{n}_e/n_e$  normalized to unity) from linear hybrid simulation of the E-GAM showing  $m = 1$  standing wave. The dashed horizontal line is the elevation of the linear BES array at the time of interest. (b) Mode frequency (blue) and linear growth rate  $\gamma/\omega$  (%) (red) vs central fast ion beta  $\beta_h(0)$ .

over a wide range of fast ion beta suggests the possibility of very strong nonlinear interactions, consistent with the bursting, rapid frequency chirping and neutron drops observed in experiment. Such a response likely maintains the fast ion distribution close to marginal stability according to theory [19,27].

Unlike ideal MHD modes, the E-GAM existence is determined by the fast ion distribution which is less well known than other equilibrium profiles and is nonlinearly modified by the instability itself. However, qualitative features of the mode are robust to variations in the fast ion distribution such as the low mode frequency and the radially extended  $m = 1$  standing wave pattern. Measurements taken along a vertical array of BES channels intersecting the magnetic axis (cf. Fig. 4) reveal an inversion of the mode parity through the magnetic axis indicative of a standing wave. The location of the mode inversion in Fig. 4 tracks the location of the magnetic axis and a mode null is also observed at the point of phase inversion. The predicted peak in the mode density is expected to occur well above and below the magnetic axis. From the location of the BES measurements just above the

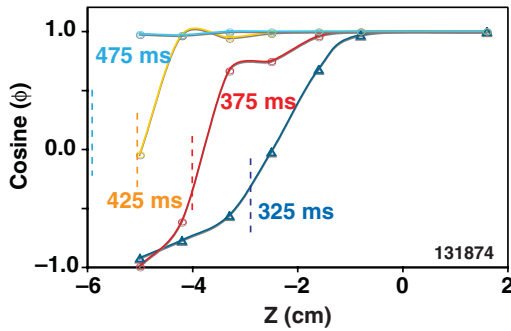


FIG. 4 (color). Cosine of the phase ( $\cos\phi$ ) of the  $n = 0$  mode vs vertical height ( $z$ ) measured along a vertical array of BES channels located at major radius  $R = 1.9$  m. The phase is shown at 4 times in a single discharge (131874), each corresponding to a different vertical height of the magnetic axis (dashed lines:  $-3$ ,  $-4$ ,  $-5$ ,  $-6$  cm, respectively). The point of phase inversion tracks the motion of the magnetic axis, indicative of an  $m = 1$  standing wave.

plasma midplane [Fig. 3(a)] we infer that the peak density fluctuation level could be as large as 10%. Further work will focus on the measurement of the peak density fluctuation level of the E-GAM in the region where the linear eigenfunction is expected to peak.

Note that an  $n = 0$  oscillation should not change the canonical angular momentum of the fast ions so that ion radial diffusion is not expected even with efficient wave-particle energy exchange. What can change is the pitch angle of the particle as it loses energy to the wave. Losses can then occur by the transit of counterpassing particles to unconfined trapped particle orbits. More speculatively, the reduction in the neutron emission could also be due to the channeling [28] of the fast ion energy to the background plasma. The combination of large linear growth rate, low mode frequency, and low radial diffusion makes it possible to couple the fast ion energy to the thermal plasma through wave dissipation mechanisms. Future nonlinear simulations will address the mechanism of fast ion loss and the possibility of channeling.

In summary, countergoing beam ions in DIII-D excite large amplitude  $n = 0$  geodesic acousticlike compressional modes in plasmas with elevated central safety factor ( $q_{\min} \geq 2$ ), relevant to steady state plasma regimes. The frequency of the modes, at about half the ideal GAM frequency, cannot be explained within the context of ideal MHD theory. A new electrostatic fluid-kinetic model reveals a robust  $n = 0$  mode, the E-GAM, which reproduces many of the features observed in experiment. The large calculated linear growth rate suggests that the instability will strongly modify the fast ion distribution to keep it close to marginal stability [19,27]. Rapid drops in the

neutron emission are indicative of intense wave-particle interactions causing beam ion loss and/or energy channeling to background plasma. A key goal of future studies is to understand the nonlinear dynamics of the instability and to confirm the predicted mode structure well above and below the plasma midplane.

This work is supported by the U.S. Department of Energy under DE-AC02-76CH03073, DE-FG03-97ER54415, DE-FC02-04ER54698, DE-FG03-01ER5461, DE-FG03-96ER54373, W-7405-ENG-48, and DE-AC05-76OR00033.

- [1] K. Ikeda, Nucl. Fusion **47**, 1213 (2007).
- [2] T. C. Luce, Nucl. Fusion **45**, S86 (2005).
- [3] A. Fasoli *et al.*, Nucl. Fusion **47**, S264 (2007).
- [4] R. B. White, *Theory of Toroidally Confined Plasmas* (Imperial College Press, London, 2006), 2nd ed.
- [5] K. L. Wong *et al.*, Phys. Rev. Lett. **66**, 1874 (1991).
- [6] W. W. Heidbrink *et al.*, Nucl. Fusion **31**, 1635 (1991).
- [7] E. D. Fredrickson *et al.*, Nucl. Fusion **46**, S926 (2006).
- [8] Y. Kusama *et al.*, Nucl. Fusion **39**, 1837 (1999).
- [9] R. Nazikian *et al.*, Phys. Plasmas **15**, 056107 (2008).
- [10] M. A. Van Zeeland *et al.*, Phys. Rev. Lett. **97**, 135001 (2006).
- [11] G. J. Kramer *et al.*, Phys. Plasmas **13**, 056104 (2006).
- [12] J. L. Luxon, Nucl. Fusion **42**, 614 (2002).
- [13] P. H. Rebut and B. E. Keen, Fusion Technol. **11**, 13 (1987).
- [14] C. J. Boswell *et al.*, Phys. Lett. A **358**, 154 (2006).
- [15] H. L. Berk, C. J. Boswell, and D. Borba *et al.*, Nucl. Fusion **46**, S888 (2006).
- [16] G. Y. Fu, following Letter, Phys. Rev. Lett. **101**, 185002 (2008).
- [17] N. Winsor, J. L. Johnson, and J. M. Dawson, Phys. Fluids **11**, 2448 (1968).
- [18] H. L. Berk, B. N. Breizman, and N. V. Petvishvili, Phys. Lett. A **234**, 213 (1997).
- [19] H. L. Berk *et al.*, Phys. Plasmas **6**, 3102 (1999).
- [20] G. McKee, K. Burrell, and R. Fonck *et al.*, Phys. Rev. Lett. **84**, 1922 (2000).
- [21] C. T. Holcomb *et al.*, Rev. Sci. Instrum. **77**, 10E506 (2006).
- [22] C. Z. Cheng and M. S. Chance, Phys. Fluids **29**, 3695 (1986).
- [23] N. N. Gorelenkov, H. L. Berk, and R. V. Budny, Nucl. Fusion **45**, 226 (2005).
- [24] G. J. Kramer *et al.*, Phys. Plasmas **13**, 056104 (2006).
- [25] S. E. Sharapov *et al.*, Phys. Rev. Lett. **93**, 165001 (2004).
- [26] R. V. Budny, Nucl. Fusion **42**, 1383 (2002).
- [27] R. G. L. Vann, H. L. Berk, and A. R. Soto-Chavez, Phys. Rev. Lett. **99**, 025003 (2007).
- [28] M. C. Herrmann and N. J. Fisch, Phys. Rev. Lett. **79**, 1495 (1997).